BULLETIN OF THE POLISH ACADEMY OF SCIENCES
TECHNICAL SCIENCES
Vol. 55, No. 2, 2007

Modelling drop dynamics on patterned surfaces

J.M. YEOMANS* and H. KUSUMAATMAJA

The Rudolf Peierls Centre for Theoretical Physics, Oxford University, 1 Keble Road, Oxford OX1 3NP, U.K.

Abstract. We present a mesoscopic model able to capture the physics of drops moving across patterned surfaces. In this model, interfaces appear naturally, and both chemical and topological patterning can be incorporated with relative ease, making it particularly suitable to study the behaviour of evolving drops. We summarise results on drop dynamics, including drops spreading on a chemically patterned surface, using a hydrophobic grid to alleviate mottle and the transition and dynamics of drops moving across a superhydrophobic surface.

Key words: lattice Boltzmann, superhydrophobic surfaces, chemically patterned surfaces, drop dynamics.

1. Introduction

From microfluidic technology to detergent design and ink-jet printing it is vital to understand the way in which drops move across surfaces. The dynamics of the drops will be affected by any heterogeneities on the surface. Until recently such disorder was usually regarded as undesirable. However with the advent of microfabrication techniques it has become possible to control the chemical and topological patterning of a substrate on micron length scales, leading to the possibility of exploring new physics and to novel applications.

There are many natural examples where surface patterning has evolved to enhance biological functions. For example several plants [1], such as the lotus, have leaves which are covered with micron-scale bumps. As a result of this topological patterning they are strongly repellent to water drops which show contact angles up to 160°. (This should be compared to more traditional ways of increasing the contact angle, surface coatings and chemical modifications of the substrate, where it is difficult to achieve an angle of more than 120°.) The evolutionary advantage to the lotus appears to be the easy run-off which helps to clean the leaves of the plant.

Another example is the Namibian desert beetle which collects water on its back from a fog-laden wind [2]. The beetle's back is bumpy and covered with alternating hydrophilic and hydrophobic regions. Large drops of water condense onto the hydrophilic bumps. The size of the drops then allows them to roll against the wind into the beetle's mouth.

It is becoming increasingly easy to fabricate similar surfaces, with micron-scale regions of different wettability [3–5] , or with a pattern of posts [6–9] as roughness leading to superhydrophobic behaviour. Increasingly such surfaces are finding industrial applications. For example, hydrophobic regions can be constructed to act as chemical valves confining drops of fluid until a sufficiently large force is applied and hydrophilic channels etched onto a surface have been used as templates for ink-jet printing of electronic circuits.

However, many fundamental questions remain about the way in which drops move across patterned surfaces. For example, superhydrophobic surfaces can show both high contact angle and fast run-off and the connection between these properties is not fully resolved. We would like to understand more fully how chemical patterning can control drop motion and whether superhydrophobic surfaces can be helpful in reducing drag in microchannels. This review summarises recent work on a mesoscopic model that is allowing us to investigate questions like these. We first summarise the model and then describe results for chemically and topologically patterned surfaces in section 3 and 4 respectively. We summarise and discuss areas for future research in Section 5.

2. The model

The model needs first to describe the equilibrium properties of the drop, such as liquid-gas coexistence, surface tension and contact angles. As we are working on micron-length scales we can use a continuum Landau free energy, which is minimised in equilibrium:

$$\Psi = \int_V (\psi_b(n) + \frac{\kappa}{2}(\partial_\alpha n)^2)dV + \int_S \psi_s(n_s)dS. \quad (1)$$

$\psi_b(n)$ is a bulk free energy term which gives two coexisting phases. A simple example is the free energy corresponding to the van der Waals equation of state

$$\psi_b(n) = p_c(\nu_n + 1)^2(\nu_n^2 - 2\nu_n + 3 - 2\beta\tau_w)\,, \quad (2)$$

where $\nu_n = (n - n_c)/n_c$, $\tau_w = (T_c - T)/T_c$ and n, n_c, T, T_c and p_c are the local density, critical density, local temperature, critical temperature and critical pressure of the fluid respectively. β is a constant typically chosen to be 0.1. This choice of free energy leads to two coexisting bulk phases of density $n_c(1 \pm \sqrt{\beta\tau_w})$.

*e-mail: halim@thphys.ox.ac.uk

The second term in Eq. (1) models the free energy associated with any interfaces in the system; κ controls the liquid-gas surface tension and the width of the interface via $\gamma = (4\sqrt{2\kappa p_c}(\beta\tau_w)^{3/2}n_c)/3$ and $\xi = \sqrt{(\kappa n_c^2)/(4\beta\tau_w p_c)}$ [10].

The last term describes the interaction between the fluid and the solid surface. For example, following Cahn [11], the surface energy density can be taken as $\psi_s(n) = -\phi\, n_s$ where n_s is the value of the density at the surface. The strength of the surface interaction ϕ is related to the contact angle θ of a drop on the surface by [10]

$$\phi = 2\beta\tau_w\sqrt{2p_c\kappa}\ \mathrm{sgn}(\frac{\pi}{2}-\theta)\sqrt{\cos\frac{\alpha}{3}(1-\cos\frac{\alpha}{3})}\,, \quad (3)$$

where $\alpha = \cos^{-1}(\sin^2\theta)$ and the function sgn returns the sign of its argument.

The hydrodynamics of the drop is described by the continuity and the Navier-Stokes equations

$$\begin{aligned} \partial_t n + \partial_\alpha(nu_\alpha) = 0\,, \quad (4)\\ \partial_t(nu_\alpha) + \partial_\beta(nu_\alpha u_\beta) = -\partial_\beta P_{\alpha\beta} \\ +\nu\partial_\beta[n(\partial_\beta u_\alpha + \partial_\alpha u_\beta + \delta_{\alpha\beta}\partial_\gamma u_\gamma)] + na_\alpha\,, \end{aligned}$$

where $\mathbf{u}$, $\mathbf{P}$, ν, and $\mathbf{a}$ are the local velocity, pressure tensor, kinematic viscosity, and acceleration respectively. (The Einstein summation convention over repeated indices is assumed.) The pressure tensor $\mathbf{P}$ is calculated from derivatives of the free energy [10]

$$\begin{aligned} P_{\alpha\beta} &\equiv \left[\partial_\beta n\frac{\partial}{\partial(\partial_\alpha n)} - \delta_{\alpha\beta}\right](\psi_b - \mu_b n + \frac{\kappa}{2}(\partial_\gamma n)^2) \\ &= (p_b(n) - \frac{\kappa}{2}(\partial_\alpha n)^2 - \kappa n\partial_{\gamma\gamma}n)\delta_{\alpha\beta} \\ &+ \kappa(\partial_\alpha n)(\partial_\beta n)\,, \quad (5)\\ p_b(n) &= p_c(\nu_n+1)^2(3\nu_n^2 - 2\nu_n + 1 - 2\beta\tau_w). \end{aligned}$$

The term $\mu_b n$ is a Lagrange multiplier imposing mass conservation. For $\mathbf{u} = 0$, achieving mechanical equilibrium $\partial_\alpha P_{\alpha\beta} = 0$ is equivalent to minimising the free energy.

Finally, we impose a no slip boundary condition $\mathbf{u} = 0$ on the surfaces. Although there is evidence for increased local slip on hydrophobic surfaces [12] this is still on the nm level and so would not show up on the scale of these simulations. It is also important to note that the three phase contact line is able to move even with a no slip boundary condition on the velocity. This is because the interface has a finite width which allows an evaporation-condensation mechanism. References [10,13–19] discuss the dynamics of contact line motion in diffuse interface models in more detail.

We used a lattice Boltzmann algorithm [5,10,20] to solve Eqs. (4) and (5) to obtain the results reported here, but other numerical approaches would be equally applicable.

3. Chemical patterning

In this Section, we describe how (regular) chemical patterning can influence the dynamics of micron-length liquid drops. In the first part, we look at a drop spreading on a chemically patterned surface. For a homogeneous surface, the final state is unique: the drop will form a spherical cap with a contact angle equals to the Young's angle [19]. This is not the case for heterogeneous surfaces: there can be more than one metastable drop configuration and the final morphology of the drop depends heavily on the initial conditions of the system.

We then in the second part consider a drop driven by an external body force and study the competition between this and the capillary forces. We choose a simple volume term for the body force (modelling, for example, gravity).

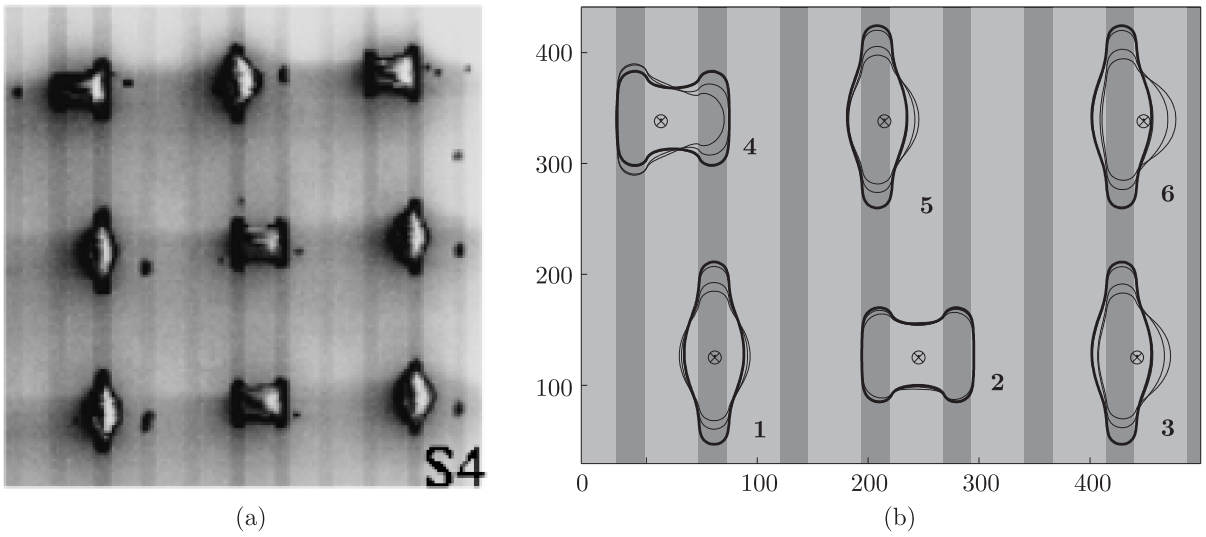

(a) (b)

Fig. 1. Drop spreading on a chemically striped surface. (a) Scanning electron micrographs of inkjet drops. (b) Numerical simulations of drops hitting the surface at various impact points indicated by encircled crosses. For each drop the bold and faint lines represent the extent of the drop at equilibrium and at intermediate times, respectively. Relatively hydrophilic and hydrophobic stripes appear dark and pale, respectively. The figures are taken after Ref. 5

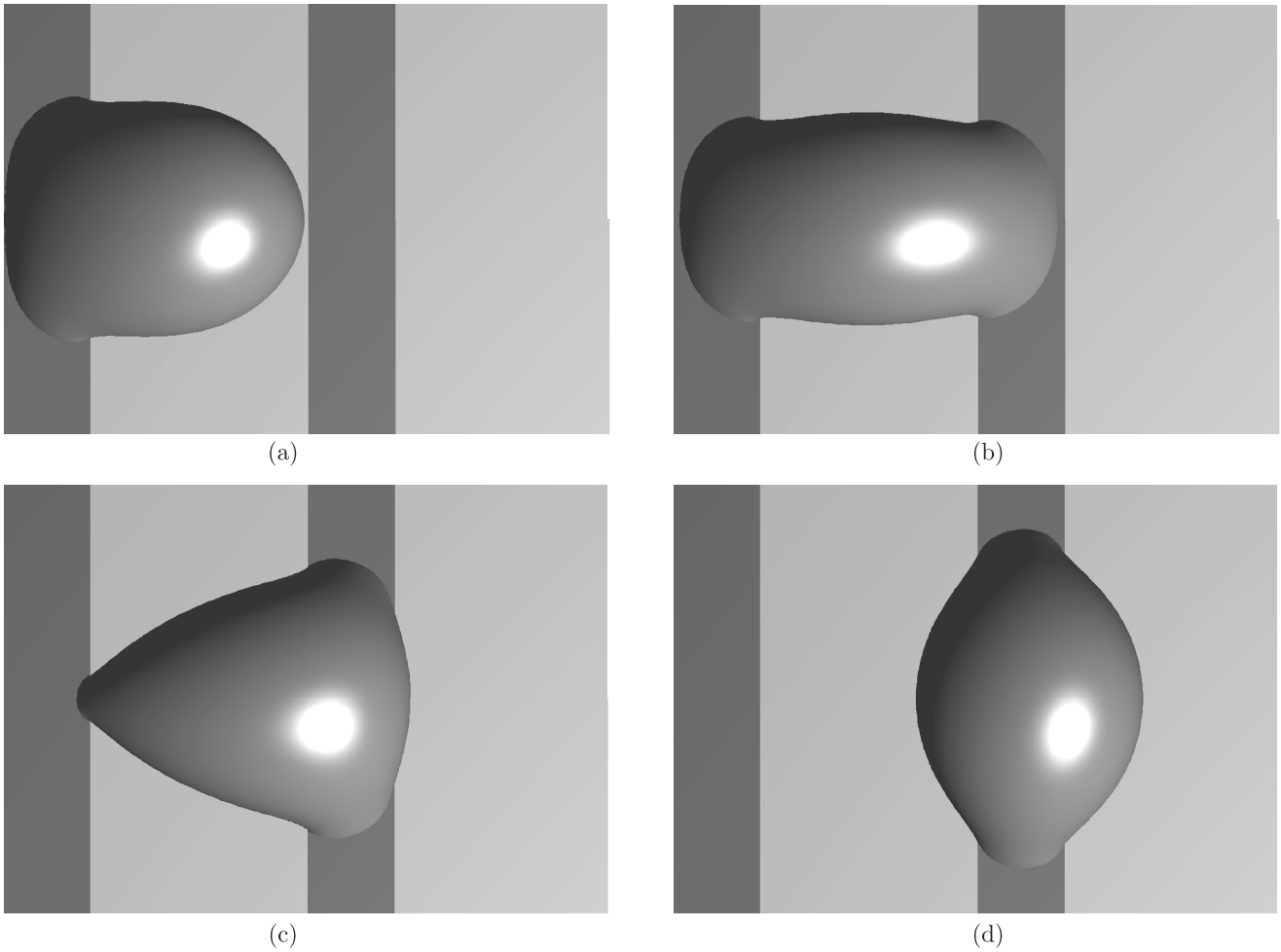

Fig. 2. Drop moving across a chemically striped surface. The evolution of the drop shape is shown in frames (a)–(d). Hydrophilic and hydrophobic stripes appear dark and pale, respectively. The figures are taken after Ref. 23

We end Section 3 by providing an example where chemical patterning may be applied to solve industrial problems. In the third part we show how a (relatively) hydrophobic grid can be used to alleviate mottle [21] in ink-jet printing. Other possible applications are numerous. For example, Darhuber et. al. discussed the use of patterned surface as printing plates [4] and Kusumaatmaja et. al. showed how chemical patterning can be used to control drop size and polydispersity [22].

3.1. Spreading on a chemically striped surface. Figure 1(a) shows experimental results for ink drops jetted onto a surface patterned with relatively hydrophilic and hydrophobic stripes with contact angles 5° and 64° and widths 26 μm and 47 μm respectively. The drop volume was chosen such that the final drop radius was the same order as that of the stripes. Note that there are two distinct final drop shapes, which we shall denote butterfly and diamond.

To understand the final drop shape we ran simulations matching the surface tension, viscosity, contact angles, stripe widths, impact velocities and drop volume to the experimental system. Simulation and physical parameters are related by choosing a length scale L_o, a time scale T_o, and a mass scale M_o appropriately [23,24]. A simulation parameter with dimensions $[L]^{n1}[T]^{n2}[M]^{n3}$ is multiplied by $L_o^{n1}\, T_o^{n2}\, M_o^{n3}$ to give the physical value.

The results are shown in Fig. 1(b). The faint lines show the time evolution of the (base of) the drop and the solid lines its final shape. As in the experiments both the butterfly and diamond drops are seen. The simulations enabled us to show that this occurs because the final drop shape is selected by the initial impact position and velocity. If the drop can reach two neighbouring hydrophilic stripes as it spreads it will reach the butterfly configuration, if not it will retract back to the diamond pattern spanning a single stripe. Both states are free energy minima but one is a metastable minimum: which one is sensitive to the exact choice of the physical parameters.

3.2. Dynamics on a chemically striped surface. In Fig. 2 we present simulation results showing how a drop moves across a similar, chemically striped, surface when pushed by a constant body force (such as gravity). The contact angles of the stripes are now 60° (dark grey) and 110° (light grey). The drop shape changes from a diamond

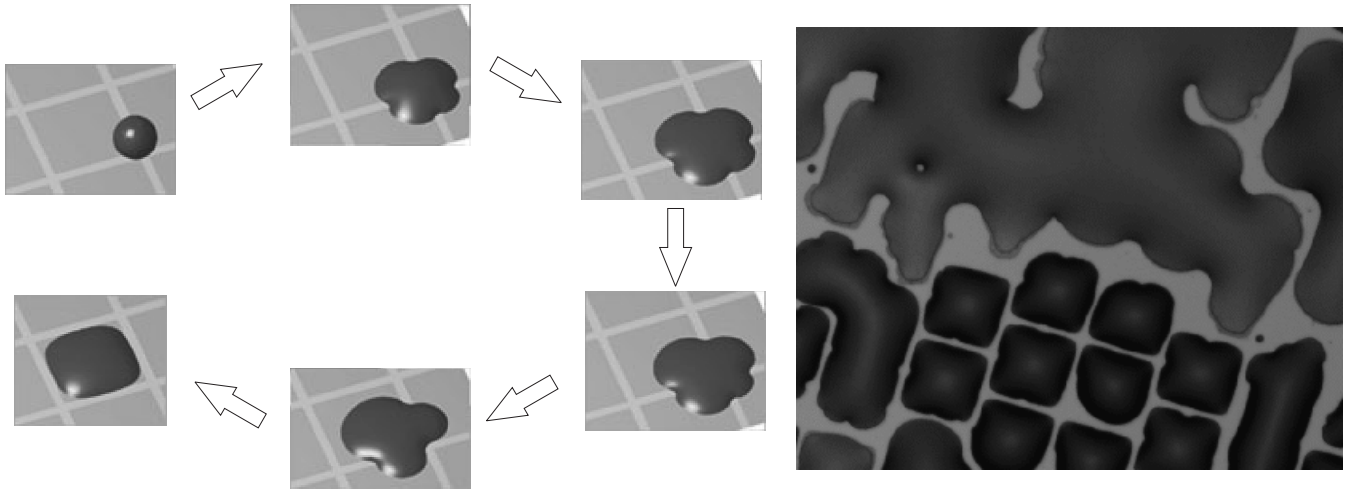

(a) (b)

Fig. 3. Control of drop position using chemical patterning. (a) Time evolution of drops jetted onto substrates patterned by grids. Relatively hydrophobic and hydrophilic areas are light grey stripes (65° and dark grey areas (5°) respectively. (b) Inkjet drops were jetted onto a substrate and cured: (top) homogeneous and (bottom) patterned. The figures are taken after Ref. 24

to a butterfly shape and back again (Fig. 2(a-d)). Let us assume the drop is initially in a diamond configuration (Fig. 2(d)). Due to the Poiseuille flow field, the drop is pushed forward onto the hydrophobic region. Its velocity decreases because of the dewetting force at the hydrophobic stripe. If the external body force is small, the drop velocity will fall to zero, the drop will be pinned, and the steady-state drop shape will look similar to Fig. 2(a). For the parameters we consider here, however, the drop is just able to channel to the next hydrophilic stripe. The effective capillary force at the chemical border then starts to take charge and the drop accelerates and wets the next hydrophilic stripe. The drop now has a butterfly shape (Fig. 2(b)), which here corresponds to the peak of an energy barrier between two diamond shapes on successive hydrophilic stripes. It then becomes more advantageous for the drop to spread along the new hydrophilic stripe in the direction perpendicular to the force rather than to continue to move along the substrate. Hence, the diamond configuration is re-formed and the oscillations repeat.

3.3. Using chemical patterning to control drop positioning. In a printed image a patch of colour is produced by jetting drops in a regular, square array. The closer the drops the more intense the colour of the patch appears to the eye. To achieve a solid colour the aim is that drops jetted at a distance apart comparable to their diameter should coalesce and form a uniform covering of ink. However, in practice, randomness in the positions at which the drops land, combined with surface imperfections, often lead to local coalescence and the formation of large, irregular drops with areas of bare substrate between them as shown in the upper part of Fig. 3(b). Such configurations are likely to lead to poor image quality, called mottle [21].

Figure 3(a) shows how this problem can be overcome by using a grid of (relatively) hydrophobic chemical stripes to control the equilibrium shape, the position, and the dynamic pathway of spreading drops thus allowing their relative positions to be tuned.

The drop has an initial radius of 15 μm and the substrate has contact angle 5°. The hydrophobic grid has stripes of width 6 μm, separated by 66 μm, and contact angle 65°. The simulation shows that the drop is confined even when its initial point of impact is close to the corner of a square.

An experiment presenting a similar situation is shown in Fig. 3(b). The ink drops have a radius $R = 30$ μm and they are jetted in a 50 μm × 50 μm array. In the upper part of the figure there is no hydrophobic grid and a mottled final configuration is observed. The lower part of Fig. 3(b) carries hydrophobic stripes of 5 μm width forming squares of side 40 μm. The drops now form a more regular array determined by the grid. (We note that each drop covers four grid squares, as the drop radius to square side length ratio is larger than in the simulations.)

4. Superhydrophobic surfaces

4.1. Introduction. We now consider surfaces that are patterned with an array of posts as shown in Fig. 4(b) and (c). When the surfaces are intrinsically hydrophobic, that is the flat surface contact angle is larger than 90°, the macroscopic contact angle of a drop on the patterned substrate increases to, in certain cases, close to 180° [6–9] . On such superhydrophobic surfaces drops can either lie in a suspended state on top of the posts or a collapsed state filling the interstices between them. In the suspended state the (averaged) macroscopic contact angle is given by the Cassie-Baxter equation [25]

$$\cos\theta_{CB} = f\cos\theta_e - (1-f) \tag{6}$$

where f is the solid (area) fraction of the substrate and θ_e is the equilibrium contact angle of the flat surface. Essen-

tially the Cassie-Baxter equation averages over the cosines of the contact angles of the posts (θ_e) and the space between them (180°). In the collapsed state the corresponding formula is due to Wenzel [26]:

$$\cos\theta_W = r\cos\theta_e \tag{7}$$

where r is a roughness factor, the area by which the liquid-solid contact area is increased by the presence of the posts. These formulae correspond to minimising the free energy of the drop under the assumption that the drop covers a large number of posts.

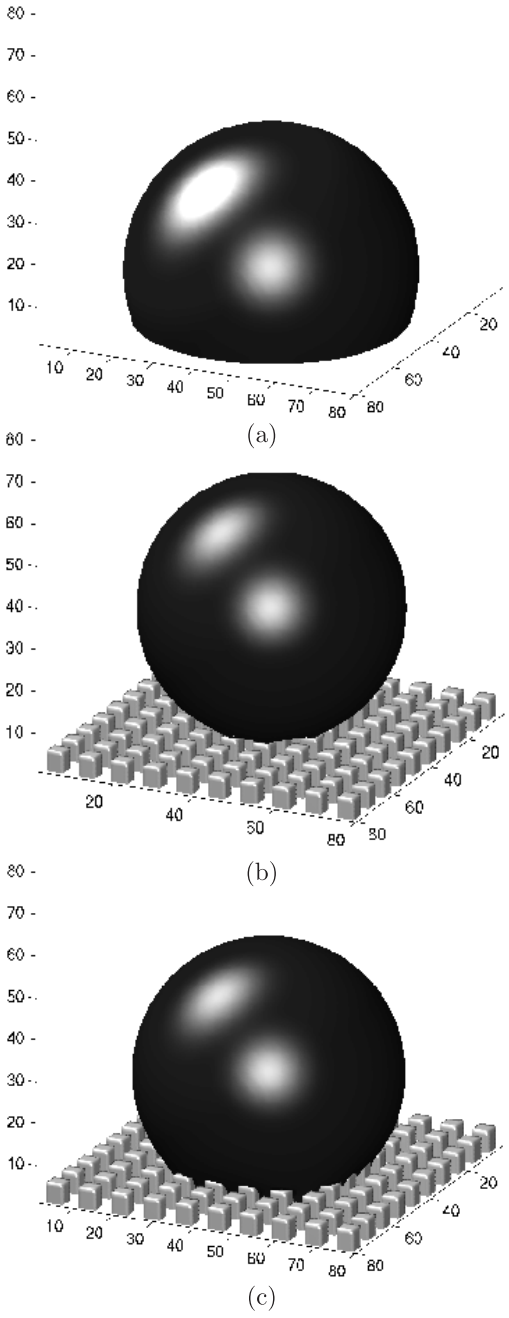

Fig. 4. Final states of a spreading drop. (a) The substrate is flat and homogeneous. (b) The substrate is decorated with posts and the drop is in the suspended state. (c) Same geometry as (b) but the drop is in the collapsed state. The figures are taken after Ref. 20

Fig. 4 shows simulation results for the final state of a drop of radius $R = 30$ spreading on a smooth (Fig. 4(a)) and a superhydrophobic surface (Fig. 4(b) and (c)). A contact angle $\theta_e = 110^o$ is set on every surface site. The resultant macroscopic contact angles in the simulations are 110°, 156° and 130° for the flat surface, suspended drop and collapsed drop respectively. The values for the suspended and collapsed drop are compatible with the ones obtain from the Cassie-Baxter and Wenzel formulae, but are not exactly the same. There are two reasons why this occurs. First, the drop only covers a finite (and small) number of posts in the simulations. Second, the surface inhomogeneities result in the existence of multiple local free energy minima, not just that prescribed by the Cassie-Baxter or Wenzel formulae. This can cause pinning of the contact line and lead to values of contact angles which depend not only on the thermodynamic variables describing the state of the drop, but also on the path by which that state was achieved. This phenomenon is known as contact angle hysteresis [6,27–33].

4.2. Transition between the Wenzel and Cassie-Baxter states. Both the collapsed and suspended superhydrophobic states can be thermodynamically stable with the phase boundary between them depending on the intrinsic contact angle and substrate geometry [34]. However, the suspended drop is often observed as a metastable state. As the drop penetrates the grooves, the area of contact between liquid and solid increases. Because the substrate is hydrophobic, this creates a free energy barrier hindering the transition. Work must be provided, by an impact velocity or gravity say, to allow it to proceed.

Our simulation allows us to follow the transition pathway. We consider a spherical drop of radius $R = 30$ initially just touching the top of the posts. A gravitational field is turned on at time $t = 70000$, and turned off at time $t = 200000$. Figure 5 shows cross sections of the drop as it undergoes the transition from the suspended to the collapsed state.

The drop first touches the susbtrate at its centre. Once this has occured the free energy barrier is overcome and it is favourable for the drop to quickly wet the rest of the surface as it is replacing two interfaces, solid-gas-liquid by a simple solid-liquid interface. Recent experiments have shown that reducing the size of a drop can also lead to a lowering of the free energy barrier and can induce a transition from the suspended to collapsed state [35].

4.3. Dynamics on superhydrophobic surfaces. Finally we comment on the way in which drops move across superhydrophobic surfaces. We have performed simulations [36] on drops pushed across superhydrophobic surfaces by a Poiseuille flow field. We found that, for drops suspended on the surfaces, there was an increase in velocity of about 50% as the number of posts is decreased to zero. We further showed that the main contribution to this effect is from the position of the drop in the Poiseuille

flow field. As the number of posts is decreased the contact angle increases and hence the drop lies, on average, further from the surface. Thus it is subjected to a higher velocity field and moves more quickly.

For collapsed drops the situation was very different. Here, as posts were introduced, they impeded the drop and its velocity fell. For a large number of posts, as the drop was pushed, it preferred to revert to the suspended state.

This is consistent with the results in the literature that a drag reduction $\sim 40\%$ can be obtained for drops on surfaces with micron-scale posts [37–41]. However, it does not explain the apparent ease with which a drop placed on a superhydrophobic surface starts to move. Further experimental and numerical investigations are needed to explore drop dynamics on superhydrophobic surfaces.

5. Conclusions

We have presented a mesoscopic model that allows us to study the statics and dynamics of drops spreading and moving across patterned surfaces. In the model interfaces appear naturally and there is no need for interface tracking. This makes it a powerful tool to study the behaviour of evolving drops, espcially when the surface geometry is complicated, as shown in the cases considered in this paper. Furthermore, the wetting properties of the liquid can be easily implemented as a boundary condition on the fluid density.

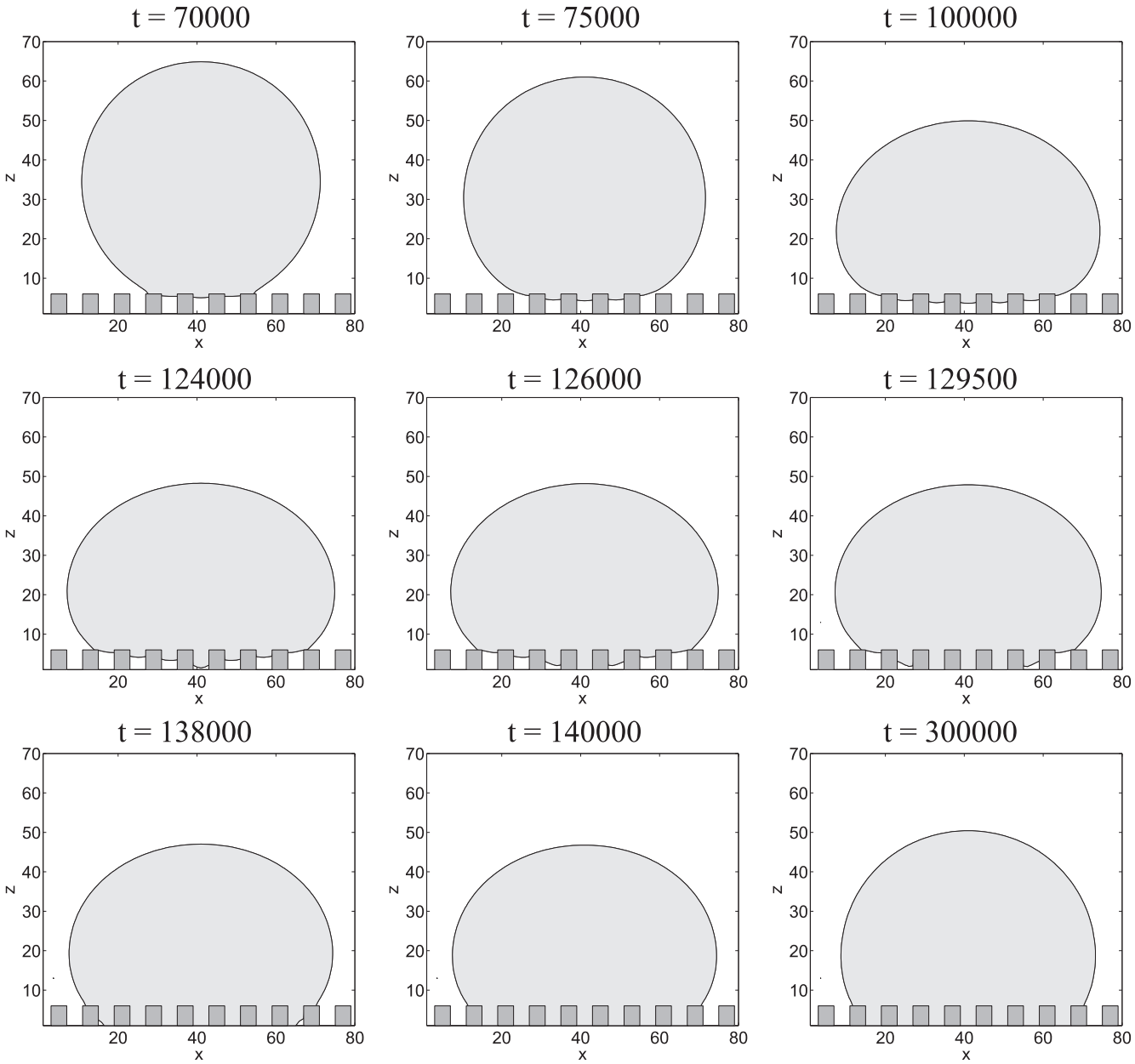

Fig. 5. Transition from a suspended to a collapsed state. These cuts are vertical cross sections across the centre of the domain where the dark grey areas are the posts and pale grey represents liquid regions.The figures are taken after Ref. 20

However, the model we solve does include approximations to make it numerically tractable and it is important to be aware of these. The model presented here is limited to isothermal systems. Moreover the contact line moves too quickly. This is because, as with all mesoscale, two-phase fluid simulations, the interface is too wide so that it can be resolved on the computational grid. Moreover the liquid-gas density ratio is limited to < 5 to avoid instabilities. The effect of this is that, given a set of input physical parameters, the simulation drop moves more quickly than a real drop. This can be accounted for by rescaling time by a constant factor. Simulation and experimental data then agree well in all the cases we have considered so far.

Other authors have used lattice Boltzmann algorithms to solve related models investigating the movement of liquids across patterned surfaces. The main difference with the approach described here is in the details of the thermodynamics. For example, Zhang and Kwok [42] replaced the square gradient interaction by a non local term and used an exponentially decaying potential (with length scale $\sim$ one lattice spacing) to mimic the fluid–wall interaction. Benzi et. al [18] started from a chosen form of the interparticle interaction.

The directions for future research are numerous. We are currently studying hysteresis on patterned surfaces. This turns out to be a very complicated problem with the contact angle hysteresis depending sensitively on the details of the surface patterning and the direction in which the interface is trying to move. One pertinent question is whether it is possible to define a sensible limit which would correspond to microscopic and random disorder on the substrate.

Recent careful experiments [43] have probed the changes in shape of a drop rolling down as inclined plane as a function of capillary number. They found that the drop developed a corner in its trailing edge and then, as the capillary number increased further, left behind a trail of small drops. We should like to investigate the extent to which the simulations can give quantitative agreement with these results.

The internal fluid motion of the drop is also of great interest: liquid drops can slip, slide and roll on a surface [44] depending on the parameters of the system. Apart from the fundamental interest in understanding what determines the motion, this is also important from a practical point of view. Recently, several authors (e.g. [45]) have suggested the use of droplets as microreactors in microfluidic devices. Since the objective here is to obtain rapid mixing, the internal fluid motion is very relevant.

We have here just considered superhydrophobic surfaces fabricated from arrays of posts. Disordered surface layers of hydrophobic grains also show superhydrophobic behaviour. Moreover plants often control their wetting properties with surface inhomogeneities at two length scales or with hairy surfaces. We are in the early stages of understanding the equilibrium properties, phase transition and hydrodynamics of drops on these substrates.

We would also like to note that the approach presented here is not limited to the study of drop motion. It can immediately be applied to study many multiphase problems, such as the dewetting of thin liquid films or flow in porous media. One can also extend the model to achieve higher density ratio [47], incorporate thermal transport, or introduce colloidal particles inside the drops [48]. The latter will allow investigation of a new set of problems, from liquid marbles [46] to the self assembly of colloidal particles [49].

Acknowledgements. We thank A. Dupuis, J. Léopoldès, G. McHale and D. Quéré for useful discussions. HK acknowledges support from a Clarendon Bursary.

References

[1] W. Barthlott and C. Neinhuis, "Purity of the sacred lotus, or escape from contamination in biological surfaces", *Planta* 202 (1), 1–8 (1997).

[2] A.R. Parker and C. R. Lawrence, "Water capture by a desert beetle", *Nature* 414 (6859), 33–34 (2001).

[3] H. Gau, S. Herminghaus, P. Lenz, and R. Lipowsky, "Liquid morphologies on structured surfaces: From microchannels to microchips", *Science* 283 (5398), 46–49 (1999).

[4] A.A. Darhuber, S.M. Troian, S.M. Miller, and S. Wagner, "Morphology of liquid microstructures on chemically patterned surfaces", *J. Appl. Phys.* 87 (11), 7768–7775 (2000).

[5] J. Léopoldès, A. Dupuis, D. G. Bucknall, and J. M. Yeomans, "Jetting micron-scale droplets onto chemically heterogeneous surfaces", *Langmuir* 19 (23), 9818–9822 (2003).

[6] D. Öner and T. J. McCarthy, "Ultrahydrophobic surfaces. Effects of topography length scales on wettability", *Langmuir* 16 (20), 7777–7782 (2000).

[7] D. Quéré, "Non-sticking drops", *Rep. Prog. Phys.* 68 (11), 2495–2532 (2005).

[8] J. Bico, C. Marzolin, and D. Quéré, "Pearl drops", *Europhys. Lett.* 47 (2), 220–226 (1999).

[9] B. He, N.A. Patankar, and J. Lee, "Multiple equilibrium droplet shapes and design criterion for rough hydrophobic surfaces", *Langmuir* 19 (12), 4999–5003 (2003).

[10] A.J. Briant, A.J. Wagner, and J.M. Yeomans, "Lattice Boltzmann simulations of contact line motion. I. Liquid-gas systems", *Phys. Rev. E* 69 (3), 031602 (2004).

[11] J.W. Cahn, "Critical-point wetting", *J. Chem. Phys.* 66 (8), 3667–3672 (1977).

[12] C. Cottin-Bizonne, J.-L. Barrat, L. Bocquet, and E. Charlaix, "Low-friction flows of liquid at nanopatterned interfaces", *Nature Mat.* 2 (4), 237–240 (2003).

[13] A.J. Briant and J.M. Yeomans, "Lattice Boltzmann simulations of contact line motion. II. Binary fluids", *Phys. Rev. E* 69 (3), 031603 (2004).

[14] P. Seppecher, "Moving contact lines in the Cahn-Hilliard theory", *Int. J. Eng. Sci.* 34 (9), 977–992 (1996).

[15] D. Jacqmin, "Contact-line dynamics of a diffuse fluid interface", *J. Fluid Mech.* 402, 57–88 (2000).

[16] H.Y. Chen, D. Jasnow, and J. Vinals, "Interface and con-

tact line motion in a two phase fluid under shear flow", *Phys. Rev. Lett.* 85 (8), 1686–1689 (2000).

[17] J.F. Zhang and D.Y. Kwok, "Lattice Boltzmann study on the contact angle and contact line dynamics of liquid-vapor interfaces", *Langmuir* 20 (19), 8137–8141 (2004).

[18] R. Benzi, L. Biferale, M. Sbragaglia, S. Succi, and F. Toschi, "Mesoscopic modeling of a two-phase flow in the presence of boundaries: the contact angle", *Phys. Rev. E* 74 (2), 021509 (2006).

[19] A. Dupuis and J. M. Yeomans, "Lattice Boltzmann modelling of droplets on chemically heterogeneous surfaces", *Fut. Gen. Comp. Sys.* 20 (6), 993–1001 (2004).

[20] A. Dupuis and J.M. Yeomans, "Modeling droplets on superhydrophobic surfaces: Equilibrium states and transitions", *Langmuir* 21 (6), 2624–2629 (2005).

[21] N.P. Sandreuter, "Predicting print mottle – a method of differentiating between 3 types of mottle", *Tappi J.* 77 (7), 173–182 (1994).

[22] H. Kusumaatmaja and J.M. Yeomans, "Controlling drop size and polydispersity using chemically patterned surfaces", *Langmuir* 23 (2), 956–959 (2007).

[23] H. Kusumaatmaja, J. Léopoldès, A. Dupuis, and J. M. Yeomans, "Drop dynamics on chemically patterned surfaces", *Europhys. Lett.* 73 (5), 740–746 (2006).

[24] A. Dupuis, J. Léopoldès, and J. M. Yeomans, "Control of drop positioning using chemical patterning", *Appl. Phys. Lett.* 87 (2), 024103 (2005).

[25] A.B.D. Cassie and S. Baxter, "Wettability of porous surfaces", *Trans. Faraday Soc.* 40, 546–551 (1944).

[26] R.N. Wenzel, "Resistance of solid surfaces to wetting by water", *Ind. Eng. Chem.* 28 (8), 988–994 (1936).

[27] L.W. Schwartz and S. Garoff, "Contact-angle hysteresis on heterogeneous surfaces", *Langmuir* 1 (2), 219–230 (1985).

[28] J.F. Joanny and P.G. de Gennes, "A model for contact angle hysteresis", *J. Chem. Phys.* 81 (1), 552–562 (1984).

[29] R.E. Johnson and R.H. Dettre, "Contact angle hysteresis. I. Study of an idealized rough surface", *Advan. Chem. Ser.* 43, 112–135 (1964).

[30] R.E. Johnson and R.H. Dettre, "Contact angle hysteresis. III. Study of an idealized heterogeneous surface", *J. Phys. Chem.* 68 (7), 1744–1750 (1964).

[31] C. Huh and S.G. Mason, "Effects of surface-roughness on wetting (theoretical)", *J. Coll. Interf. Sci.* 60 (1), 11–38 (1977).

[32] J.F. Oliver, C. Huh, and S.G. Mason, "Resistance to spreading of liquids by sharp edges", *J. Coll. Interf. Sci.* 59 (3), 568–581 (1977).

[33] W. Chen, A.Y. Fedeev, M.C. Hsieh, D. Oïer, J. Youngblood, and T. J. McCarthy, "Ultrahydrophobic and ultralyophobic surfaces: some comments and examples", *Langmuir* 15 (10), 3395–3399 (1999).

[34] C. Ishino, K. Okumura, and D. Quéré, "Wetting transitions on rough surfaces", *Europhys. Lett.* 68 (3), 419–425 (2004).

[35] M. Reyssat, J.M. Yeomans, and D. Quéré, *Europhys. Lett.*, (2007), (to be published).

[36] A. Dupuis, and J.M. Yeomans, "Dynamics of sliding drops on superhydrophobic surfaces", *Europhys. Lett.* 75 (1), 105–111 (2006).

[37] J. Ou, B. Perot, and J. Rothstein, "Laminar drag reduction in microchannels using ultrahydrophobic surfaces", *Phys. Fluids* 16 (12), 4635–4643 (2004).

[38] E. Lauga and H. A. Stone, "Effective slip in pressure-driven Stokes flow", *J. Fluid Mech.* 489, 55–77 (2003).

[39] J.R. Philip, "Flows satisfying mixed no-slip and no-shear conditions", *Z. Angew. Math. Phys.* 23 (3), 353–372 (1972).

[40] C. Cottin-Bizonne, J.L. Barrat, L. Bocquet, and E. Charlaix, "Low-friction flows of liquid at nanopatterned interfaces", *Nature Mat.* 2 (4), 237–240 (2003).

[41] M. Sbragaglia, R. Benzi, L. Biferale, S. Succi, and F. Toschi, "Surface roughness-hydrophobicity coupling in microchannel and nanochannel flows", *Phys. Rev. Lett.* 97 (20), 204503 (2006).

[42] J.F. Zhang, B. Li, and D.Y. Kwok, "Mean-field free-energy approach to the lattice Boltzmann method for liquid-vapor and solid-fluid interfaces", *Phys. Rev. E* 69 (3), 032602 (2004).

[43] T. Podgorski, J.-M. Flesselles, and L. Limat, "Corners, cusps, and pearls in running drops", *Phys. Rev. Lett.* 87 (3), 036102 (2001).

[44] S.R. Hodges, O.E. Jensen, and J.M. Rallison, "Sliding, slipping and rolling: the sedimentation of a viscous drop down a gently inclined plane", *J. Fluid Mech.* 512, 95–131 (2004).

[45] Y.C. Tan, J.S. Fisher, A.I. Lee, V. Cristini, and A.P. Lee, "Design of microfluidic channel geometries for the control of droplet volume, chemical concentration, and sorting", *Lab Chip* 4 (4), 292–298 (2004).

[46] P. Aussillous and D. Quéré, "Properties of liquid marbles", *Proc. R. Soc. A* 462 (2067), 973–999 (2006).

[47] T. Inamuro, T. Ogata, S. Tajima, and N. Konishi, "A lattice Boltzmann method for incompressible two-phase flows with large density differences", *J. Comp. Phys.* 198 (2), 628–644 (2004).

[48] K. Stratford, R. Adhikari, I. Pagonabarraga, and J.-C. Desplat, "Lattice Boltzmann for binary fluids with suspended colloids", *J. Stat. Phys.* 121 (1–2), 163–178 (2005).

[49] M. Schnall-Levin, E. Lauga, and M. P. Brenner, "Self-assembly of spherical particles on an evaporating sessile droplet", *Langmuir* 22 (10), 4547–4551 (2006).